

## Density functional calculation of the interaction between carbon nanotube and picric acid

Magdi Hassan Saad<sup>1\*</sup>, Mohammed A. H. Khalafalla<sup>1</sup><sup>1</sup>Department of Physics, Faculty of Science, Taibah University, Yanbu, 46423, Saudi Arabia;DOI: <https://doi.org/10.56293/IJASR.2022.5507>

IJASR 2023

VOLUME 6

ISSUE 2 MARCH - APRIL

ISSN: 2581-7876

**Abstract:** Removing the picric acid from the liquid is a significant process for an environmentally safe liquid phase. We have conducted systematic calculations based on density functional theory (DFT) to assess the affinity of carbon nanotube (CNT) towards collecting the picric acid. The picric-CNT interacting structure revealed desirable electrochemical properties in comparison with some other biological molecules (e.g. hydroxychloroquine). Such a finding suggests the stability of the picric-CNT, indicating that the CNT has a strong affinity towards purging the environment from the picric acid. The stability of the picric-CNT structure is further verified by the absence of the negative frequency modes from the IR spectrum.

**Keywords:** Picric acid; Carbon nanotube; environment cleaning; DFT calculation

## 1. Introduction

As mentioned by Faraz et al [1], picric acid (inset of Fig. 1(a)) is regarded as a dangerous environmental pollutant that is produced, for instance, in the leather industry. Therefore, the risk of it being widespread in the environment is very likely, threatening human health. Researchers have linked the causes of some diseases to exposure to picric acid [2]. Thus, significant efforts are made towards removing and detecting the picric [3]. Practically there are different strategies for treating picric acid including oxidation/precipitation, adsorption, electrochemical passivation, and some biological treatment, to mention a few [4]. The most common removal method is the economically attractive adsorption method. Additionally, this method is efficient, feasible, and rapid [5].

Hence, the task is to pursue an efficient adsorbent for collecting the picric acid. Such adsorbent should be sufficiently selective as well as have a significant adsorption capacity. It should be durable in an aggressive environment [6]. For instance, Faraz et al [1] have synthesized a C60 nanocomposite-based picric acid detector with remarkable selectivity and sensitivity towards picric acid. Moreover, Azadfar et al [7] have experimentally demonstrated the utilization of carbon nanotubes for the removal of picric acid from aqueous solutions. In general, such works indicate the adaptability of carbon-based systems as efficient absorbers for collecting picric acid from a given environmental media. Specifically, carbon nanotubes (CNTs, [8]) can be regarded as one of the materials of choice for the removal of contaminations from the environment [9].

In this work, we would like to contribute to the ongoing efforts pursuing methods for picric acid removal by systematically calculating the interaction between CNT and picric acid. The study of the electrochemical properties and structural stability of the picric-CNT coupled structure may give an insight into the affinity of CNT towards removing the picric acid, specifically from the aqueous media. Our calculations are based on Density-Functional-Theory (DFT [10]) and show that picric-CNT has desirable electrochemical properties in comparison with some other biological molecule (e.g. hydroxychloroquine [11], which is merely chosen for this comparison study owing to its common availability as an organic molecule). We have also investigated the structural stability of the picric-CNT compound via infrared calculations, which show no negative frequency modes, validating the structural stability.

## 2. Materials and methods

### 2.1 Method for calculations based on density functional theory (DFT)

The structure for the picric acid (C<sub>6</sub>H<sub>3</sub>N<sub>3</sub>O<sub>7</sub>) calculation was obtained from PubChem [12] under PubChem CID of 6954. This is followed by converting the structure into a 3-dimensional (3D) "XYZ" format utilizing the Openable

software[13]. For the carbon nanotube (CNT) generation, we used the TubeGen online server [14] followed by passivation of the dangling carbon bonds at the edges of the CNT by H atoms. The combined picric-CNT structure was formed using VESTA software [15].

The density-functional-theory (DFT, [10]) based calculations concerned with the energetics, polarizability, infrared (IR) vibrational frequencies, and the optimization of the configuration of the picric-CNT interacting structure have been carried out using the ORCA program[16]which implements the hybrid functional B3LYP [17]and def2-SVP basis sets[18] in the water phase. The water phase calculation was performed using the conductor polarizable continuum model (CPCM) [19].

The numerical frequency (rather than the analytical one) for the vibrational frequency calculation (Infrared spectra) was implemented. Regarding the calculations of the vibrational frequencies, we observed no negative (imaginary) frequencies, suggesting the mechanical stability of our optimized structures. For all structures the charge was zero and multiplicity ( $M = 2S + 1$ , where S is the total spin) was 1.

### 3. Results and discussion

#### Calculations based on Density Functional Theory (DFT)

##### Electrochemical properties

The analysis of the frontier orbitals (Highest Occupied Molecular Orbitals (HOMO) and Lowest Unoccupied Molecular Orbital (LUMO)) is important for assessing the structure of the optimized picric-CNT (CNT  $\equiv$  carbon nanotube) properties. It has been reported that the degree of reactivity between interacting molecular species can be associated with the energy gap between HOMO and LUMO[20]–[22].

Figures 1(b) and 1(c) show the HOMO and LUMO as blue and red meshes around the optimized picric-CNT structures. We observed that the HOMO and LUMO spread wide along this structure. A quantitative analysis of the picric-CNT reactivity is possible via the following parameters[21]: absolute hardness,  $\eta = E_{\text{gap}}/2$ , and absolute electronegativity,  $\chi = -(E_{\text{HOMO}} + E_{\text{LUMO}})/2$ , where  $E_{\text{gap}}$  is the difference between the energy of the HOMO,  $E_{\text{HOMO}}$ , and LUMO,  $E_{\text{LUMO}}$ . Softer structure tends to have smaller  $E_{\text{gap}}$  and, hence, are more polarizable. These calculated parameters are listed in the early, the polarizability (in Ha a.u.) for our structure is quite large relative to that ( $\sim 220$  Ha) for the hydroxychloroquine (which is a drug molecule that has been used for comparative purposes). We have calculated the properties of the hydroxychloroquine with the same calculation setting as that used for our picric-CNT structure.

One of the desirable molecular structure is its high electronegativity,  $\chi = -(E_{\text{HOMO}} + E_{\text{LUMO}})/2$ . Again, our picric-CNT structure has higher  $\chi$  and that for the hydroxychloroquine ( $\sim 3.5$  eV).

##### Infra Red (IR) absorption calculation

Figure 2 shows the theoretical IR absorption spectrum for the drug molecules calculated using OR the CA program. The discussion of the Infrared (IR) data involves the verification of the structural ability from the absence of imaginary frequencies (as seen fig. 2) in the IR spectrum. Thus, we confirmed that the picric-CNT (CNT  $\equiv$  carbon nanotube) compound shown in Fig. 1(a) was structurally stable.

IR calculation also reveals the types of molecular bonding, which can be shown qualitatively as follows. The transmission valleys (or absorption peaks) around frequencies (or wavenumbers)  $> 2500$   $\text{cm}^{-1}$  in figure 2 are disassociated with O-H, C-N, and C-H bonds available for picric-CNT (picric  $\equiv \text{C}_6\text{H}_3\text{N}_3\text{O}_7$ ) as is evident from the Figure 1(a). While for  $< 2000$   $\text{cm}^{-1}$  the transmission valleys are mostly due to absorption of the spectrum by C=C and C=N type of bonds. No clear transmission feature is observed between these ranges, which may explain the lack of C $\equiv$ C bonds in our structure. Fig. 2 clearly shows that the absorption peaks (i.e. transmission valleys) are more pronounced CNT than for the picric due to the dominance of the CNT atomic components.

## Conclusion

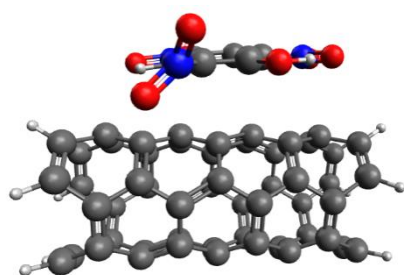
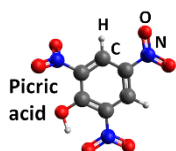
The search and development of CNT compounds displaying picric acid purging activities is of significant concern to environmental science and technology. Our systematic DFT calculations on picric-CNT interacting structure revealed desirable electrochemical properties in comparisons with the hydroxychloroquine drug molecule. Such finding suggests the stability of the picric-CNT, indicating that the CNT has strong affinity towards purging the environment from the picric acid. The stability of the picric-CNT structure is further verified from the absence of the negative frequency modes from the IR spectrum.

## References

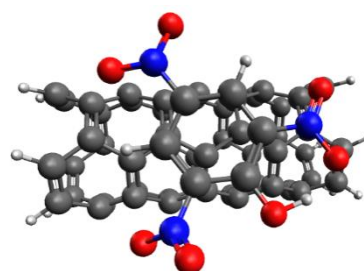
1. M. Faraz, M. Shakir, and N. Khare, "Highly sensitive and selective detection of picric acid using a one pot biomolecule inspired polyindole/CdS nanocomposite," *New J. Chem.*, vol. 41, no. 13, pp. 5784–5793, 2017.
2. M. Nipper, R. S. Carr, J. M. Biedenbach, R. L. Hooten, and K. Miller, "Fate and effects of picric acid and 2, 6-DNT in marine environments: Toxicity of degradation products," *Mar. Pollut. Bull.*, vol. 50, no. 11, pp. 1205–1217, 2005.
3. Y. Song, X. Pang, J. Chen, Y. Lu, J. Xie, and Y. Ye, "Determination of picric acid using micro CdS crystal-modified glassy carbon electrode," *Int. J. Environ. Anal. Chem.*, vol. 100, no. 9, pp. 957–967, 2020.
4. Z. Doroudi and M. R. Jalali Sarvestani, "Boron nitride nanocone as an adsorbent and sensor for Ampicillin: A Computational Study," *Chem. Rev. Lett.*, vol. 3, no. 3, pp. 110–116, 2020.
5. B. Agarwal *et al.*, "Sensitivity and selectivity of switchable reagent ion soft chemical ionization mass spectrometry for the detection of picric acid," *J. Phys. Chem. A*, vol. 118, no. 37, pp. 8229–8236, 2014.
6. H. Uslu and G. Demir, "Adsorption of picric acid from aqueous solution by the weakly basic adsorbent amberlite IRA-67," *J. Chem. Eng. Data*, vol. 55, no. 9, pp. 3290–3296, 2010.
7. M. Azadfar, H. Tahermansouri, and M. Qomi, "The picric acid removal from aqueous solutions by multi-walled carbon nanotubes/EDTA/carboxymethylcellulose nanocomposite: Central composite design optimization, kinetic, and isotherm studies," *J. Chin. Chem. Soc.*, vol. 68, no. 11, pp. 2103–2117, 2021.
8. M. S. Dresselhaus, G. Dresselhaus, P. Eklund, and A. Rao, *Carbon nanotubes*. Springer, 2000.
9. V. K. Upadhyayula, S. Deng, M. C. Mitchell, and G. B. Smith, "Application of carbon nanotube technology for removal of contaminants in drinking water: a review," *Sci. Total Environ.*, vol. 408, no. 1, pp. 1–13, 2009.
10. R. G. Parr, "Density functional theory of atoms and molecules," in *Horizons of quantum chemistry*, Springer, 1980, pp. 5–15.
11. D. J. Browning, "Pharmacology of chloroquine and hydroxychloroquine," in *Hydroxychloroquine and chloroquine retinopathy*, Springer, 2014, pp. 35–63.
12. S. Kim *et al.*, "PubChem 2019 update: improved access to chemical data," *Nucleic Acids Res.*, vol. 47, no. D1, pp. D1102–D1109, 2019.
13. N. M. O'Boyle, M. Banck, C. A. James, C. Morley, T. Vandermeersch, and G. R. Hutchison, "Open Babel: An open chemical toolbox," *J. Cheminformatics*, vol. 3, no. 1, p. 33, 2011.
14. "TubeGen Online - v3.4." <https://turin.nss.udel.edu/research/tubegenonline.html> (accessed Feb. 24, 2023).
15. K. Momma and F. Izumi, "VESTA: a three-dimensional visualization system for electronic and structural analysis," *J. Appl. Crystallogr.*, vol. 41, no. 3, pp. 653–658, 2008.
16. F. Neese, "Software update: the ORCA program system, version 4.0," *Wiley Interdiscip. Rev. Comput. Mol. Sci.*, vol. 8, no. 1, p. e1327, 2018.
17. I. Y. Zhang, J. Wu, and X. Xu, "Extending the reliability and applicability of B3LYP," *Chem. Commun.*, vol. 46, no. 18, pp. 3057–3070, 2010.
18. F. Weigend and R. Ahlrichs, "Balanced basis sets of split valence, triple zeta valence and quadruple zeta valence quality for H to Rn: Design and assessment of accuracy," *Phys. Chem. Chem. Phys.*, vol. 7, no. 18, pp. 3297–3305, 2005.
19. Y. Takano and K. Houk, "Benchmarking the conductor-like polarizable continuum model (CPCM) for aqueous solvation free energies of neutral and ionic organic molecules," *J. Chem. Theory Comput.*, vol. 1, no. 1, pp. 70–77, 2005.
20. I. Fleming and others, *Frontier orbitals and organic chemical reactions*. Wiley, 1977.
21. R. G. Pearson, "Absolute electronegativity and hardness correlated with molecular orbital theory," *Proc. Natl. Acad. Sci.*, vol. 83, no. 22, pp. 8440–8441, 1986.
22. R. G. Parr and R. G. Pearson, "Absolute hardness: companion parameter to absolute electronegativity," *J. Am. Chem. Soc.*, vol. 105, no. 26, pp. 7512–7516, 1983.

Table 1. The calculated electrochemical properties for picric-CNT structure

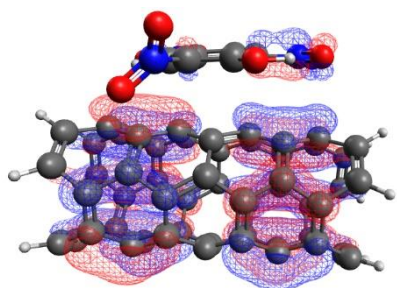
$E_{\text{HOMO}}$ (eV)	-4.68
$E_{\text{LUMO}}$ (eV)	-3.509
$\eta_{\square}$ (eV)	0.5855
$\chi_{\square}$ (eV)	4.0945
Polarizability (Ha)	1423.66



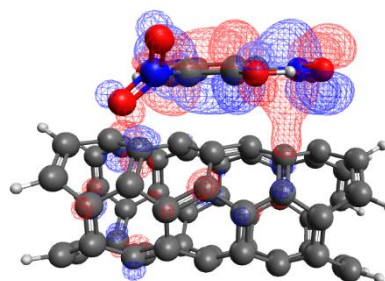
(a)



(b)



(c)



(d)

(a) Side view of the geometrically optimized picric acid – carbon nanotube interacted structure. Inset: picric acid cal structure,  $C_6H_3N_3O_7$  (b) Top view of the same structure in (a). (c) The isosurface (red and blue mesh) of the O (Highest Occupied Molecular Orbital) around the same structure in (a). (d) The isosurface (red and blue mesh) LUMO (Lowest Unoccupied Molecular Orbital) around the same structure in (a).

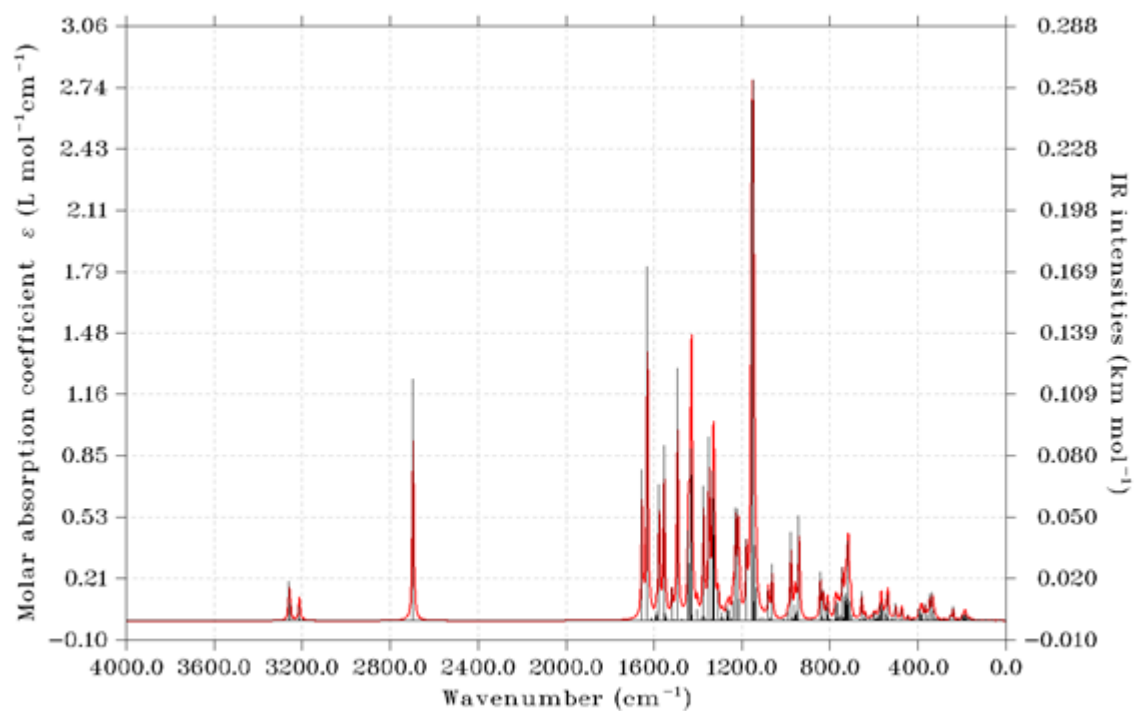


Figure 2. Theoretical Infrared transmission spectra for the optimized structure in Fig. 1(a).